

Carrier g-factors in quasi-two-dimensional graphites

A. S. Kotozonov

State Research Institute for Graphite-Based Structural Materials

(Submitted 19 March 1987)

Zh. Eksp. Teor. Fiz. 93, 1870–1878 (November 1987)

Electron paramagnetic resonance in quasi-two-dimensional graphites is used to measure the g -factor in the temperature range 3.8–1000 K. Most of the EPR absorption is due to carriers whose g -factor has an appreciable anisotropy (Δg_c) connected with the two-dimensional orbital motion of the electrons. The magnitude and temperature dependence of Δg_c are determined by the fraction of the unpaired electrons occupying states in the vicinity where the valence and conduction band are in contact. Increasing the density of the electrically active structure defects or of a boron impurity in graphite leads to a shift of the Fermi level into the interior of the valence band and to a sharp decrease of Δg_c . It is proposed to explain the behavior of Δg_c in quasi-two-dimensional graphites, especially at low temperature, by taking into account the effective “smearing,” due to scattering of carriers by defects, of the density of states in the vicinity of the contact between the bands.

INTRODUCTION

The first investigations of EPR signals of the single-crystal graphite¹ have shown that the observed paramagnetic resonance is due mainly to proper carriers that appear as a result of the small overlap of the filled and empty bands in the vicinity of the corners of the reduced Brillouin zone. Owing to the small spin-orbit coupling in carbon ($\approx 2.2 \cdot 10^{-4}$ eV, Ref. 2), the g -factor in graphite differs little from that of the free electron ($g_0 = 2.0023$), although the deviation Δg from g_0 is easily observed and depends substantially on the direction of the constant magnetic field H relative to the hexagonal c -axis of the graphite. It was established¹ that $\Delta g_c = g_c - g_0 = 4.37 \cdot 10^{-2}$ for $H \parallel c$ and $\Delta g_a = g_a - g_0 = 3 \cdot 10^{-4}$ for $H \perp c$ (or $H \parallel a$). These experimental data were later satisfactorily explained in Ref. 2.

For graphites with structure defects or specially doped with impurities, the theoretical estimates^{2–4} of Δg_c differ noticeably from the experimental data, especially at low temperatures.^{4–6} The most instructive in this respect are quasi-two-dimensional graphites (QTDG), whose graphite layers have a sufficiently regular structure in the absence of azimuthal order between the layers (for example pyrocarbons obtained at 2100 °C Refs. 4–6). Owing to the weak interlayer interaction, the band overlap in QTDG is lifted, and at low temperatures the carriers should be the impurities. According to the existing theories,^{2,3} at $T < T_0/2$, where T_0 is the degeneracy temperature of the impurity carriers, Δg_c should decrease exponentially with decrease of T , whereas the observed Δg_c either increases or flattens out.

In the present study the g factor was measured in a wide range of temperatures (3.8–1000 K), using QTDG with different densities of the intrinsic structural defects, and also QTDG specially doped with boron. The experimental data are compared with the present theories. To eliminate the existing disparities, it is proposed to take scattering of electrons by defects into account, effects that lead to “smearing” of the energy spectrum near the singular conical point in the band model of two-dimensional graphite (TDG).

The QTDG samples were highly textured “pure” pyrocarbons (PC) and borated pyrocarbons (BPC), obtained by deposition of the products of pyrolysis of hydrocarbons on a flat substrate at 2100 °C. According to the x-ray structure

analysis, the samples had a two-dimensionally ordered structure with interlayer distance $d = 0.343$ nm.

The values of the g -factor were determined the EPR signals from plates measuring 2×1 and 5×0.15 mm at plate orientation in the magnetic field $H \parallel Z$ and $H \perp Z$, where Z is the normal to the plane of the plate and coincides with the most probable direction of the c -axes of the individual crystallites (the PC axial-texture axis).

Registration of the EPR spectra of graphite materials is usually made complicated by the substantial and inhomogeneous broadening of the absorption line, on account of structural and textural inhomogeneities, and especially on account of the “oxygen effect.”^{7,8} The samples selected for the investigations were therefore those with a minimum linewidth ΔH at close values of Δg , which attested to uniformity of the samples or to small dimensions of the inhomogeneities compared with the diffusion path length of the unpaired electron during the spin-lattice relaxation time (complete translational averaging of the g -factor). To eliminate the “oxygen effect,” the measurements at low temperatures were carried in purified helium, and at high temperatures with an excess chlorine pressure.⁹ The EPR signal was measured with a Varian E-12 spectrometer equipped with the appropriate temperature attachments. At low temperature, the most suitable for this purpose is the ESB-9 temperature-varying unit. The resonant-magnetic-field strength was measured with a type E-500 NMR gaussmeter, and the microwave field frequency was measured with an HP-5342A frequency meter. The calculated g factor was corrected for the influence of the skin effect on the line shape and for the shift of the resonance field in accordance with Dyson’s theory.¹⁰ The temperature-measurement error in the investigated range did not exceed 2%, and the absolute error of the g factor did not exceed $5 \cdot 10^{-5}$.

EXPERIMENTAL RESULTS AND DISCUSSION

Owing to the non-ideal texture of the crystallites in the pyrocarbons, the values of $g_z(H \parallel Z)$ and $g_x(H \perp Z)$ measured for the plates can differ noticeably from the values of g_c and g_a of the individual crystallites. If $\Delta g/g$ is small, however, and for complete translational averaging of the g -factor, the measured values are easily expressed in terms of g_c

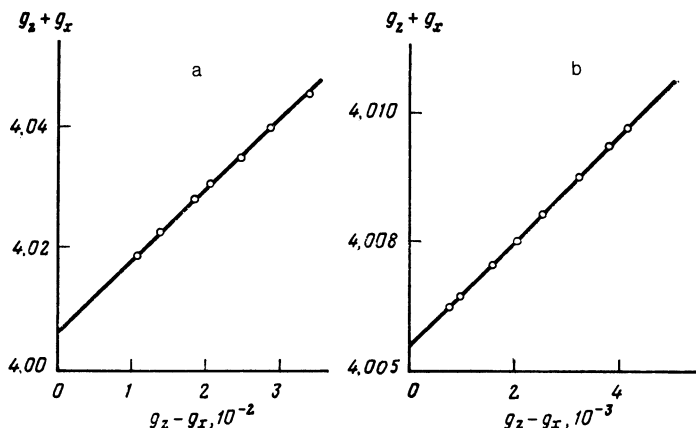


FIG. 1. Comparison of $(g_z + g_x)$ with $(g_z - g_x)$ for samples PC-3 (a) and BPC-2 (b).

and g_a and in terms of the texture parameters $\langle \sin^2 \theta \rangle$:

$$g_z = g_c - (g_c - g_a) \langle \sin^2 \theta \rangle, \quad g_x = g_a + \frac{1}{2}(g_c - g_a) \langle \sin^2 \theta \rangle. \quad (1)$$

Here θ is the angle between the axial-texture axis **Z** and **c** axes of the individual crystallites, and the angle brackets denote averaging over the sample volume. To find $\langle \sin^2 \theta \rangle$ one can use another useful expression obtained from (1):

$$g_z + g_x = 2g_a + (g_z - g_x)(2 - \langle \sin^2 \theta \rangle)/(2 - 3\langle \sin^2 \theta \rangle). \quad (2)$$

In view of the two-dimensional character of the electron motion, the value of g_a should not be influenced by the state of the system of free carriers, and hence by the measurement temperature. On the contrary, the contribution of the component g_c to the measured values of g_z and g_x is temperature dependent. It is therefore easy enough to determine both $\langle \sin^2 \theta \rangle$ and g_a from the correlations between $(g_z + g_x)$ and $(g_z - g_x)$. As a rule, at $T > 77$ K (i.e., when the influence of the low concentration of the localized centers on the EPR signal can be neglected, the experimental points for all the samples can be approximated with high accuracy by straight lines (Fig. 1) in accordance with Eq. (2). The relatively small values of ΔH of the EPR signal permit a reliable estimate of $\langle \sin^2 \theta \rangle$, g_a , and g_c . The determined values of these quantities for the investigated samples are listed in Table I, together with the measured g_a for quasi-single-crystal graphite (QSCG) with practically ideal texture. The close values of g_a of the investigated samples attest to the applicability of the chosen approach to the investigation of these materials.

Knowing $\langle \sin^2 \theta \rangle$, we easily determine from Eqs. (1) the value of g_c and hence the shift of the g factor $\Delta g = g_c - g_0$ in the investigated temperature range. Data on the dependence of Δg_c on T for pure PC are shown in Fig. 2. It is important to note that, at a chosen temperature, Δg_c is

lower the larger the defect content of the two-dimensional layer and the larger the ensuring density of the hole carriers. At the same time, the character of the temperature dependence of Δg_c is practically the same for all the investigated PC, viz., Δg_c increases as the temperature is lowered to 50–20 K, and the decreases as $T \rightarrow 0$. A similar dependence of Δg_c on T in 77–300 K range was observed for analogous carbon materials in a number of studies,^{5,6} but found no acceptable explanation so far.

Since the PC chosen by us had a QTDG structure, it is possible to apply to them primarily the model of TDG with linear dispersion.¹¹ McClure¹³ developed within the framework of this model a g -factor c theory according to which the shift Δg_c is given by:

$$\Delta g_c = \frac{\alpha \lambda}{2k_B T \ln(2 \operatorname{ch}(\eta/2))} \times \left[\frac{3ma^2\gamma_0^2}{4\hbar^2 k_B T \operatorname{ch}^2(\eta/2)} + \alpha \operatorname{th}(\eta/2) \operatorname{sgn} \eta \right], \quad (3)$$

where α is the probability coefficient for the $3d$ functions in the π band, λ is the spin-orbit interaction constant of $3d$ electrons, m is the electron mass, $a = 0.246$ nm is the translation constant in the graphite layer, γ_0 is a two-dimensional band parameter equal to ≈ 3 eV (Ref. 12), $\eta = E_F/k_B T$ is the reduced Fermi level, E_F is the Fermi level, and sgn is the “signum” symbol. The energy is reckoned from the point of tangency of the valence band and the conduction band towards the conduction band.

Knowing the value of the Fermi level E_{F0} of the degenerate system of carriers, we can find the dependence of Δg_c on T by determining η from the electroneutrality condition, which takes of the TDG band model the form

TABLE I. Values of the temperature parameter $\langle \sin^2 \theta \rangle$, the EPR linewidth ΔH , and the g -factor components (g_a, g_c) of the investigated samples. (The values of ΔH and g_c are given for $T = 300$ K).

	PC-1	PC-2	PC-3	BPC-1	BPC-2	BPC-3	BPC-4	QSCG
$\langle \sin^2 \theta \rangle$	0.147	0.12	0.15	0.12	0.15	0.205	—	~0
$\Delta H(\mathbf{H} \perp \mathbf{Z})$, Oe	2.3	2.3	1.5	2.2	2.1	0.95	0.57	3.1
$\Delta H(\mathbf{H} \parallel \mathbf{Z})$, Oe	5.1	3.4	2.4	3.4	2.2	0.95	0.53	6.1
g_a	2.0028	2.0030	2.0029	2.00275	2.0028	2.0028	2.0027	2.0029
g_c	2.0725	2.0518	2.0266	2.0173	2.0054	2.00295	2.0024	2.0488

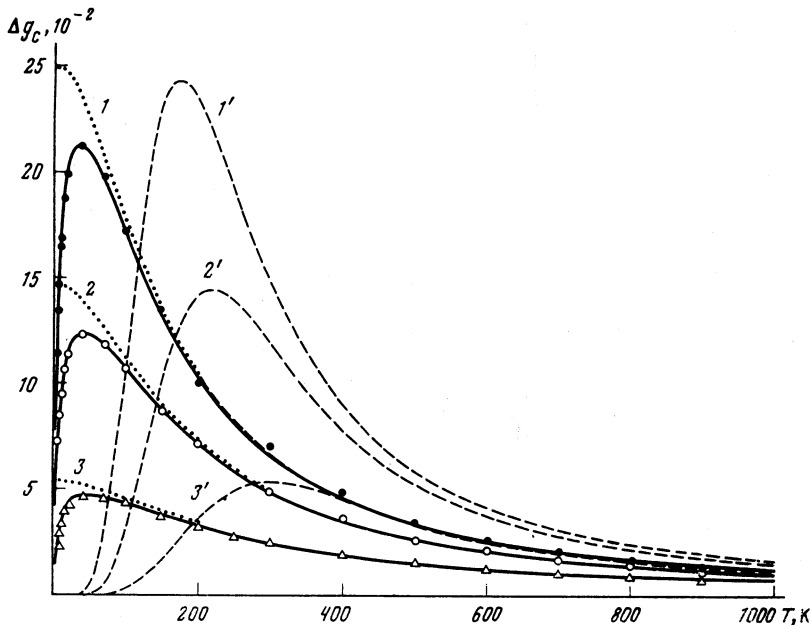


FIG. 2. Temperature dependence of Δg_c for PC. The numbers of the sets of presented data correspond to the number of the sample. Points—experiment; lines—calculation—dashed calculated in accordance with the theory of Ref. 3, dotted—with allowance for the influence of the carrier scattering from the defects on the density of states, solid—additional allowance for the localized moments. The data of Table II were used for the calculations.

$$F_1(\eta) - F_1(-\eta) = \frac{1}{2} \eta_0^{-2} \operatorname{sgn} \eta_0, \quad (4)$$

where F_1 is a Fermi index of unity index, $\eta_0 = T_0/T$, and $T_0 = E_{F0}/k_B$ is the degeneracy temperature. The value of T_0 depends on the density of the layer defects, which exhibit acceptor properties in PG. An independent estimate of T_0

$$\eta = \operatorname{sgn} \eta_0 \begin{cases} 0.36\eta_0^2 & \text{for } |\eta_0| \leq 1 \\ 0.006\eta_0^{-4} - 0.0958\eta_0^{-3} + 0.532\eta_0^{-2} - 0.08\eta_0 & \text{for } 1 < |\eta_0| < 5 \\ (\eta_0^{-2} - \pi^2/3)^{-1/2} & \text{for } |\eta_0| \geq 5 \end{cases} \quad (5)$$

As shown by calculations using Eq. (3), the theoretical dependences of Δg_c on T (Fig. 2, dashed lines) do not agree with experimental points for any reasonable variation of γ_0 and $\alpha\lambda$. The reason for this difference is, in our opinion, that the theory of Ref. 3, developed for idealized TDG, cannot be directly applied to QTDG because of effects due to carrier scattering by structure defects, which smear out the density of states in the vicinity of the conical singular point.

It was shown in a recent analysis¹³ of the diamagnetism of QTDG that the influence of scattering effects on the smearing of the density of states can be formally taken into account by introducing in lieu of T the effective temperature $T_e = T + \delta$, where

$$\delta = \frac{\hbar}{\pi k_B \tau} = \left(\frac{e^2}{2\pi\hbar} \right) \left(\frac{2T_0}{\pi\sigma_s} \right). \quad (6)$$

Here τ is the carrier relaxation time and σ_s is the two-dimensional conductance of the graphite layer. The remaining cal-

culations are carried out in the framework of the “rigid” band model of the TDG. For PG with structure defects at low temperatures, the conductance $\sigma_s = 0.45 \cdot 10^{-4} \Omega^{-1}$ and is independent of the defect density.¹¹ In this case $\delta \approx 0.5T_0$. Introduction of T_e in place of T in Eqs. (3) and (4) actually leads to a satisfactory fit of the experimental points to the calculated curves (Fig. 2, dotted lines), although at $T < 100$ K the difference between calculation and experiment remains noticeable. This difference will be shown below to be due to the contribution made to the EPR signal by localized paramagnetic centers whose g -factor is less than g_c , while the susceptibility increase as $T \rightarrow 0$ in accordance with the Curie law. At $T > 200$ K the agreement between experiment and calculation by Eq. (3) is good enough. Analysis of Eq. (3) has shown that for $E_F < 1$ eV the contribution of the second term is negligibly small compared with that of the first, so that in practice the only remaining fit parameter is the product $\alpha\lambda$. The best approxi-

TABLE II. Values of the parameter γ_0 , of the degeneracy temperature T_0 , of the spin-orbit coupling energy $\alpha\lambda$, of the density n (per unit graphite-layer area) of the improper hole carriers and of the localized moments N in the investigated samples.

	PC-1	PC-2	PC-3	BPC-1	BPC-2	BPC-3	BPC-4
γ_0 , eV	3.1	3.05	2.85	3.1	3.1	3.1	3.05
T_0 , K	350	435	590	1250	1950	3100	5000
$\alpha\lambda$, 10^{-5} eV	2.5	2.65	2.0	2.7	2.4	2.7	2.5
n , 10^{10} cm $^{-2}$	6.6	11	22	82	200	520	1350
N , 10^{10} cm $^{-2}$	0.15	0.22	0.33	0.36	0.3	—	—

mation of the experimental points was obtained for the parameters listed in Table II. It can be seen that the value of $\alpha\lambda$ varies in the range $(2.4-2.7) \cdot 10^{-5}$ eV. Assuming $\lambda = 2.2 \cdot 10^{-4}$ eV (Ref. 2), the probability coefficient α for the $3d$ functions in the π band is 0.1–0.12.

It must be noted that the small values of ΔH of the spectral lines (Table I) attest to the complete averaging of the g -factor over all the energy states of the carriers within the time of the spin-lattice relaxation. Thus, for example, for PC-1 change of temperature from 40 to 1000 K changes g_c by ≈ 0.2 , corresponding to a shift of the resonance field by ≈ 300 Oe, whereas the EPR line width is maintained within several oersted.

The deviation of Δg at $T < 100$ K from the values calculated in accordance with Eq. (3) is due to the presence in PC of a definite fraction of unpaired electrons localized on the defects. Owing to the strong exchange interaction between the conduction electrons and the localized paramagnetic centers, one absorption line is observed, a feature common to all graphite materials.⁷ The total electronic susceptibility should be equal to the sum of the susceptibility components, and the position of the line is determined by the averaged value of the g -factor¹⁴:

$$\bar{g} = (g_c \chi_c + g_L \chi_L) / (\chi_c + \chi_L), \quad (7)$$

where χ_c and χ_L are the respective susceptibilities of the conduction electrons and of the localized centers, and g_L is the g -factor of the localized centers. Following Ref. 14, we assume $g_L = g_0 = 2.0023$. It is easy to show then that the following relation should hold between \bar{g} and Δg :

$$\bar{g} = \Delta g_c / (1 + \chi_L / \chi_c). \quad (8)$$

Since the susceptibility of the localized centers obeys the Curie law ($\chi_L = J/T$), the difference between Δg_c and \bar{g} turns out to be temperature-dependent and reaches a maximum at low temperatures:

$$\chi_c(\Delta g_c / \bar{g} - 1) = J/T, \quad (9)$$

where $J = \mu_B^2 g_L^2 N S(S+1) / (3k_B)$, μ_B is the Bohr magneton, and S and N are respectively the spin and density of the localized moments. For QTDG with a linear dispersion law¹¹ the susceptibility χ_c of the current carriers per unit mass can be represented in the form

$$\chi_c = g_c^2 \mu_B^2 N_A k_B T_e \ln [2\text{ch}(\eta/2)] (3^{1/2} \pi \gamma_0^2 M)^{-1}, \quad (10)$$

where N_A is Avogadro's number and M is the mole of carbon. Note that here $T_e = T + \delta$ (effective temperature), whereas in (9) T is the lattice temperature.

The values of χ_c can be calculated for each sample by substituting in Eq. (10) the corresponding values of T_e and obtained by the analysis of Δg . Substituting next the calculated values of Δg_c and χ_c in and the experimental values of \bar{g} in (9), we can easily verify the validity of the expression in the low-temperature range (Fig. 3), as well as estimate the parameter J , and hence also the density N of the localized centers. Allowance for the effect of N on the exchange averaging of the g factor has made it possible to fit the experimental points to the calculated curves in the entire temperature interval (Fig. 2, solid lines).

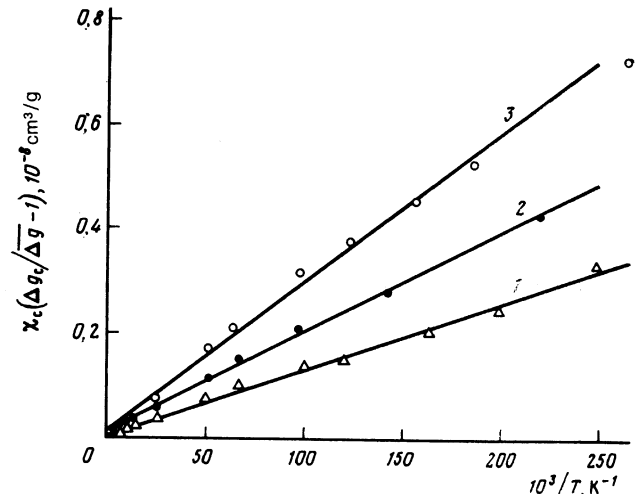


FIG. 3. Temperature dependence of $\Delta g_c / \Delta g$ for PC. The numbers on the curves are those of the samples.

Table II lists the corresponding values of the parameters for the system of carriers, and also the densities of the localized magnetic centers, with a value $S = \frac{1}{2}$ assumed for the latter. It can be seen that the density N is only a small fraction of the carrier density (<2% for PC), although the localized centers influence Δg at low temperatures quite substantially. This influence is due to the smaller value of g_L and to the increase of χ_L as $T \rightarrow 0$. The temperature dependences of the calculated values of χ_c and χ_L are shown in Fig. 4.

The carrier density and the mean free path in borated PC are determined mainly by the concentration of the boron dissolved in the lattice, with the transport cross section smaller for carrier scattering by boron ions than by structure defects. We have therefore for BPC $\sigma_s = 1.4 \cdot 10^{-4} \Omega^{-1}$ and $\delta \approx 0.17 T_0$, i.e., the effective temperature T_e is closer to T than in pure PC. Therefore at higher temperatures the experimentally observed values of Δg_c and those calculated from McClure's theory differ less for BPC than for PC. The difference between experiment and theory, however, becomes substantial at low temperatures (Fig. 5, dashed

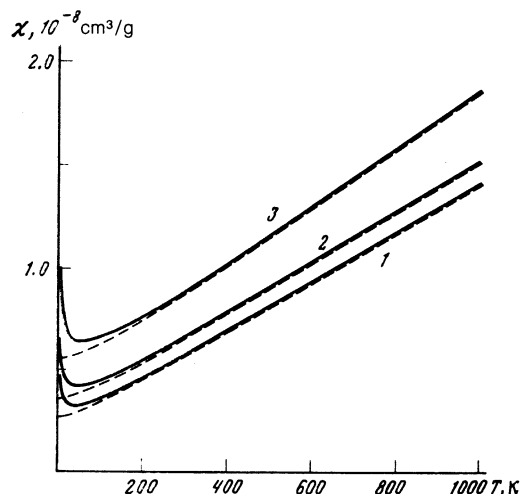


FIG. 4. Temperature dependence of the paramagnetic spin susceptibility χ for PC: dashed line—carrier susceptibility (χ_c), solid—total susceptibility of carriers and localized centers ($\chi_c + \chi_L$). The numbers on the curves are the numbers of the samples.

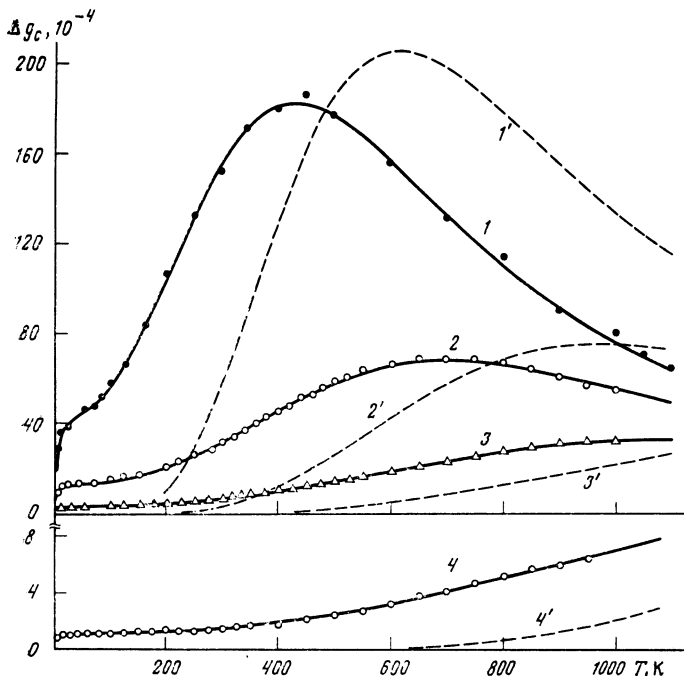


FIG. 5. Temperature dependence of Δg_c for BPC. The symbols are the same as in Fig. 2. The theoretical curves were calculated using the data of Table II.

lines). It turns out that the experimental data cannot be completely described by Eq. (3) even by introducing T_e , since the values of Δg_c observed at $T < T_0/2$ are always higher than the calculated ones. In first-order approximation this fact can be explained by assuming that the BPC contain small sections in which the electron scattering by the intrinsic structure defects remains dominant.¹³ Since one and the same narrow EPR signal line ($\Delta H \leq 1$ Oe) is observed in the investigated samples, the lengths of such sections should be shorter than the diffusion path of the electron during the spin-lattice relaxation time, thus leading to a total translational averaging of the g-factor. The agreement between the theoretical curves with experiment at all temperatures becomes good (Fig. 5, solid lines) if it is assumed that for such sections we have $\delta \approx 0.5T_0$ (just as in pure PC), and their fraction depends on the structural features of the specific sample. For the BPC described in this paper, the fractions of such sections in Samples 1, 2, 3, and 4 are respectively 17, 17, 11, and 9%.

CONCLUSION

Thus, we investigated here by EPR spectroscopy, for the first time ever, the temperature dependences of the g-factor in textured pure and specially borated pyrocarbons, whose crystal structure is that of quasi-two-dimensional graphites. It was established that the EPR signal is due primarily to current carriers, and the value of the spin susceptibility χ_c and its temperature dependence (Fig. 4) depend on the density of the impurity carriers and on the details of the electron distribution over the energy states. At low temperatures, a noticeable contribution to the EPR by localized spins is observed in PC, although their density does not exceed 2% of that of the carriers (Table II).

In QTDG the values of g_c for individual crystallites can be both higher and lower than g_c for single-crystal graphite (Table I), depending on the location of the Fermi level in the valence band, connected in turn with the density of the electrically active structural defects and impurities. Redistribution of the electrons over the energy states of the valence

band and the conduction band with change of temperature is the cause of the strong temperature dependence of g_c . The maximum of g_c (and hence Δg_c) corresponds to the temperature at which the fraction of electrons contributing to the EPR and occupying states in the vicinity of the tangency of the bands is a maximum.

For the investigated QTDG, the values of Δg_c in the entire temperature interval can be quantitatively described by modifications of Eqs. (3)–(5), in which T is replaced by an effective temperature $T_e = T + \delta$ that takes formally into account the influence of the carrier scattering from defects on the smearing of the density of states in the vicinity of the conical singularity. As $T \rightarrow 0$, the g-factor observed in PC decreases because of exchange interaction of the carriers with localized moments, for which $g_L = 2.0023$, and the paramagnetism increases in accordance with the Curie law.

On the whole, the approach described in the paper can be used for an interpretation of the EPR signal in all real carbon materials with graphite-like structure.

The author thanks V. F. Gantmakher for interest in the work and for a helpful discussion of the results.

- ¹G. Wagoner, Phys. Rev. **118**, 647 (1960).
- ²J. W. McClure and Y. Yafet, 5th Bienn. Conf. on Carbon, Buffalo, N.Y. 1962, Vol. 1, p. 22.
- ³J. W. McClure, 8th Bienn. Conf. on Carbon, Buffalo, N.Y. 1967, p. E4.
- ⁴A. S. Kotosonov, Pis'ma Zh. Eksp. Teor. Fiz. **29**, 431 (1970) [JETP Lett. **29**, 307 (1979)].
- ⁵M. Cerutti, Carbon, **9**, 391 (1971).
- ⁶K. Kawamura, S. Kaneko, and T. Tsuzuku, J. Phys. Soc. Jpn. **52**, 3936 (1983).
- ⁷T. Kotosonov, Dokl. Akad. Nauk SSSR **196**, 637 (1971).
- ⁸S. Morozowski, Carbon **17**, 227 (1979); **20**, 303 (1982).
- ⁹A. S. Kotosonov, V. S. Tverskiy, P. M. Rubinovich, and V. G. Ostronov, USSR Inventors Cert. 873078. Publ. in Byull. Izobret. No. 38, 1981.
- ¹⁰G. Feher and A. F. Kepp, Phys. Rev. **98**, 337 (1955).
- ¹¹A. S. Kotosonov, Zh. Eksp. Teor. Fiz. **86**, 995 (1984) [Sov. Phys. JETP **59**, 580 (1984)].
- ¹²R. O. Dillon, I. L. Spain, and J. W. McClure, J. Phys. Chem. Sol. **38**, 635 (1977).
- ¹³A. S. Kotosonov, Pis'ma Zh. Eksp. Teor. Fiz. **43**, 30 (1986) [JETP Lett. **43**, 37 (1986)].
- ¹⁴S. Mrozowski, Carbon **3**, 305 (1965).

Translated by J. G. Adashko